

An Improved Mellor-Yamada Level-3 Model and its Application to a Prediction of Advection Fog

Project Representative

Toshiyuki Hibiya Graduate School of Science, The University of Tokyo

Authors

Mikio Nakanishi National Defence Academy

Hiroshi Niino Ocean Research Institute, The University of Tokyo

The improved Mellor-Yamada level-3 model proposed by Nakanishi and Niino (2004, *Boundary-Layer Met.*, 112, 1-31) is further modified to be numerically stable. Validity of the modified version is tested in a regional prediction of advection fog.

In order to ensure the realizability for the improved M-Y Level-3 model and its numerical stability, restrictions are imposed, in computing stability functions, on L/q , the temperature and water-content variances, and their covariance, where L is the master length scale and $q^2/2$ the turbulent kinetic energy per unit mass. The model with these restrictions predicts vertical profiles of mean quantities such as temperature that are in good agreement with those obtained from large-eddy simulation of a radiation fog. In a regional prediction, it also reasonably reproduces a satellite-observed horizontal distribution of an advection fog.

Keywords: Turbulence closure model, advection fog

1. Introduction

Turbulence closure models of higher-order are known to often show pathological behavior, in which computation of fluxes becomes unstable and gives unphysical values. The principal cause for this is that these models do not always satisfy realizability conditions: e.g., a constraint that keeps velocity variances nonnegative. To ensure the realizability for the M-Y level-2.5 model, many researchers suggested inclusion of various restrictions and modifications on parameters involving velocity and temperature gradients and on the turbulent kinetic energy (TKE) and length scale¹⁻⁵⁾. Our improved M-Y level-3 model^{6,7)}, is incorporated with the modification by Helfand and Labraga³⁾ (hereafter HL88), which appears to be physically most plausible. HL88, however, did not consider the realizability for the level-3 model and thus the improved M-Y level-3 model requires an additional modification to avoid the possible instability mentioned above.

The first aim of the present report is to describe a scheme for imposing several restrictions on turbulent quantities such as temperature variance in order to ensure the realizability for the improved M-Y level-3 model and its numerical stability (Section 2). The second is to demonstrate an application of the model with the restrictions to a regional prediction of advection fog around the Northern Japan (Section 3).

2. Improved Mellor-Yamada Level-3 Model and Restrictions

2.1 Stability functions

According to Nakanishi and Niino⁷⁾ (hereafter NN04), the stability function S , in the turbulent diffusivity coefficients for the level-3 model can be written in terms of difference from level-2.5 model as $S = S_{2.5} + S'$, where the subscript 2.5 denotes a variable in the level-2.5 model, a prime the difference from it. The first and second terms contain the denominators, $D_{2.5}$ and D' , respectively, which both are proved to be positive in neutral stratification as a special case. Generally, however, $D_{2.5}$ and D' can vanish due to their dependencies on

$$G_M = \frac{L^2}{q^2} \left[\left(\frac{\partial U}{\partial z} \right)^2 + \left(\frac{\partial V}{\partial z} \right)^2 \right]$$

and

$$G_H = - \frac{L^2}{q^2} \frac{g}{\Theta_0} \left(\beta_\theta \frac{\partial \Theta_l}{\partial z} + \beta_q \frac{\partial Q_w}{\partial z} \right),$$

where (U, V) is the horizontal wind velocity, Θ_l the liquid water potential temperature, Q_w the total water content, $q^2/2$ the TKE per unit mass, L the master length scale, Θ_0 the potential temperature in a reference state and β_θ and β_q are constants of the condensation process⁷⁾.

2.2 Restriction on L/q

To avoid this singularity, a number of previous studies

imposed restrictions on G_H , q^2 , and $L^{1,4,5}$. HL88³⁾ introduced a limiting function α ($0 \leq \alpha \leq 1$) which corresponds to a restriction on q^2 and assures the positiveness of the above quantities. When $G_H > 0$, α guarantees positive $D_{2.5}$ and D' ³⁾. Thus, for unstable stratification, no additional restriction to HL88 is necessary. On the other hand, for a stable stratification, D' can become nonpositive and relevant singularity problem for a stable stratification has been reported on the realizability of the vertical velocity variance^{1,5)}

Here we impose a restriction on L/q as

$$\frac{L}{q} \leq \left[\frac{g}{\Theta_0} \left(\beta_\theta \frac{\partial \Theta_l}{\partial z} + \beta_q \frac{\partial Q_w}{\partial z} \right) \right]^{-1/2}, \text{ for } G_H < 0.$$

This restriction can be interpreted as $L < q/N$, where N is the buoyancy frequency, if $\Theta_v = \beta_\theta \Theta_l + \beta_q Q_w$, where Θ_v is the virtual potential temperature.

Under a stable stratification, the master length scale L tends to be limited by the buoyancy length scale L_B . Nakanishi⁶⁾ and NN04⁷⁾ adopted

$$L_B = \begin{cases} q/N, & \partial \Theta_v / \partial z \text{ and } \zeta \geq 0, \\ (1 - I_t) q/N, & \partial \Theta_v / \partial z \text{ and } \zeta < 0, \end{cases}$$

where $\zeta = z/L_M$ with the Obukhov length L_M . Note that the second condition applies to the upper part of a convective mixed layer for which the increase of TKE, I_t , due to the turbulent transport and the buoyancy production is considered. It is found that the restriction on L/q is always satisfied for $\zeta \leq 0$, but not for $\zeta < 0$, so that a modification is activated in the upper part of the mixed layer.

2.3 Restrictions on variances

As stratification becomes stable and wind shear increases, the vertical velocity variance $\langle w^2 \rangle$ decreases. Mellor and Yamada¹⁾ pointed out that the return-to-isotropy hypothesis of Rotta is valid in the range where all the normalized velocity variances are not less than 0.12, and imposed a lower bound of 0.12 only on $C_w = \langle w^2 \rangle / q^2$. Janjić⁵⁾ also considered a similar bound for C_w , except that its value is about 0.14. In the level-3 model, the dependency of the normalized velocity variances, C_w , $C_u = \langle u^2 \rangle / q^2$, and $C_v = \langle v^2 \rangle / q^2$, on C_θ , the normalized temperature variance enables any of the normalized velocity variances to become less than 0.12. Therefore we will impose the restrictions that $C_w > 0.12$ and also $C_u, C_v > 0.12$.

3. Simulations

3.1 One-dimensional simulation of a radiation fog

We first compare the performance of the improved M-Y level-3 model with the present restrictions (Model II) with that of the models in NN04 (Model I) in a one-dimensional context, by simulating a radiation fog observed in the Netherlands⁸⁾. Figure 1 shows vertical profiles of temperature obtained from LES⁷⁾, Model I, Model II, the improved

level-2.5 model⁷⁾ (Model III), and the original level-3 model except that closure constants of Kantha and Clayson⁹⁾ are used (Model O). NN04 has shown that Model I reproduces reasonably well the evolution of the mixed layer simulated by LES⁷⁾. Model II is found to give much better agreement with the temperature profiles simulated by LES; both the cold bias for the nocturnal boundary layer and the warm bias for the convective mixed layer almost disappear. This shows that the consideration of the limitations arising from model assumptions not only eliminates the inherent numerical instability but also gives a better performance.

Model III exhibits a fairly good performance comparable to Model II in the lower part of the mixed layer, but predicts a slower growth of the convective mixed layer. Note that Model O gives much worse prediction than Model III does.

3.2 Three-dimensional simulation of an advection fog

3.2.1 Regional prediction model

Model II is incorporated into a three-dimensional mesoscale hydrostatic model in the terrain-following coordinate system. The horizontal diffusivity coefficient K_h is given by

$$K_h = C_s^2 \Delta x \Delta y \left\{ 2 \left[\left(\frac{\partial U}{\partial x} \right)^2 + \left(\frac{\partial V}{\partial y} \right)^2 \right] + \left(\frac{\partial U}{\partial y} + \frac{\partial V}{\partial x} \right)^2 \right\}^{1/2},$$

where Δx and Δy are horizontal grid spacings and C_s is chosen to be 0.4¹⁰⁾. The lower-boundary conditions are determined from Monin-Obukhov similarity theory. The land-surface temperature is predicted by the force restore method, while the sea-surface temperature (SST) is fixed at NEAR-GOOS daily SST provided by JMA. The lateral-boundary condition is a radiative-nesting condition¹¹⁾. At the upper boundary, a radiative condition¹²⁾ is adopted to avoid reflections of gravity waves.

An advection fog that frequently appears around the Northern Japan in summer is simulated. The size of the computational domain is 920 km \times 920 km in the horizontal directions and 5300 m in the vertical direction. The uniform horizontal grid spacing of 10 km is used, and the vertical grid spacing varies from 20 m near the surface to 400 m above a height of 3000 m. The model is one-way nested within the Regional Spectral Model¹³⁾, whose grid point values are provided every 3 hours. A time step is set to 30 s.

3.2.2 Results

Figures 2a and 2b show a visible image of GMS-5 at 1200 JST on 5 August 1999 and a maritime wind field from QuikSCAT at about 1800 JST on the same day, respectively. Warm, moist air advected by a southerly wind was cooled from the sea surface and eventually formed a fog layer over the Pacific near Hokkaido Island.

The simulation was started at 2100 JST on 4 August 1999

using the NEAR-GOOS daily SST on 5 August. Figures 2c and 2d show horizontal distributions of liquid-water path after 15 hours and horizontal wind at 10-m height after 21 hours, respectively. The characteristics of the wind field around Hokkaido Island are reproduced reasonably well [Figures 2b and 2d]. The distribution of the fog over the Pacific is also in reasonable agreement with the satellite image, but that over the Sea of Okhotsk is erroneous [Figures 2a and 2c].

In order to examine the cause of this erroneous fog distribution over the Sea of Okhotsk, sensitivity experiments were done. Among them, two of the significant experiments are shown in Figure 3. The first experiment (Experiment A) is performed by replacing the SST with that on 10 August [Figure 3a]. During several days before 5 August, a stationary front had existed over the Sea of Okhotsk, which may have disturbed the satellite observation. Since the SST of the Sea of Okhotsk on 10 August is evaluated to be about 1-2 K

higher than that on 5 August, the fog over the Sea of Okhotsk is somewhat suppressed in Experiment A. Since the SST of the Pacific in the east of Hokkaido Island was about 0-3 K lower, on the other hand, the fog area over the Pacific expanded southward. These result in more resemblance to the satellite observation [Figure 2a].

The second experiment (Experiment B) is performed by reducing the radiative heating/cooling rate by half [Figure 3b]. For this experiment, the fog over the Sea of Okhotsk disappeared completely, although the fog area over the Pacific also was reduced. These two experiments show that, although SST is a factor affecting the formation of advection fog, the most important factor for the present case is the radiation process. Our radiation scheme^{7,15} employed a simplified longwave-radiation scheme¹⁴.

Finally, it should be mentioned that Model O with the present restrictions also predicts nearly a similar horizontal

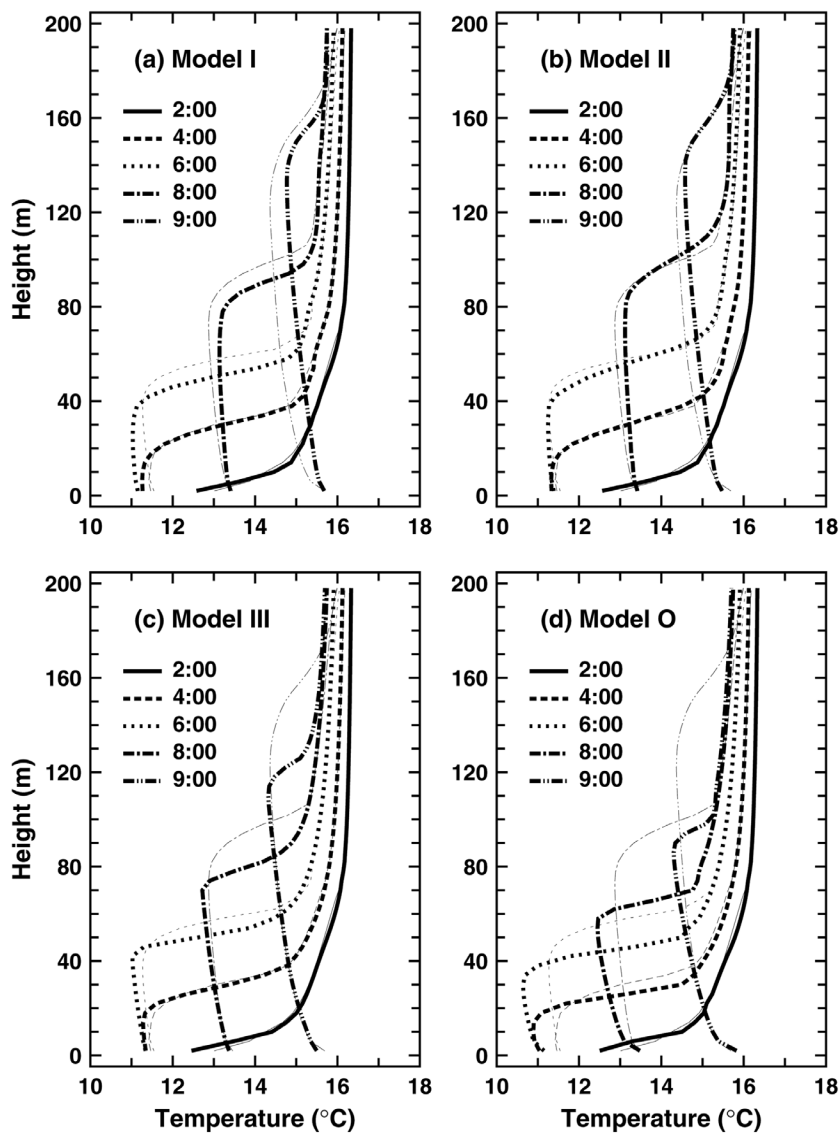


Fig. 1 Vertical profiles of temperature obtained from (a) Model I (without the present restrictions), (b) Model II (with the present restrictions), and (c) Model III, and (d) Model O. Solid, dashed, dotted, dot-dashed, and double dot-dashed lines represent the profiles at 0200, 0400, 0600, 0800, and 0900 UTC, respectively. Thin lines indicate LES results. All the results except those of Model II are extracted from NN04¹⁶.

distribution of the fog (not shown); however, Model O gives somewhat larger liquid-water content and shallower fog layer than Model II does, mainly because of the insufficient growth of the boundary layer in Model O. Since the liquid-

water content and cloud-top height affect the shortwave radiation reaching the surface and the outgoing longwave radiation, their accurate prediction is very important for daily weather forecasts and climate predictions.

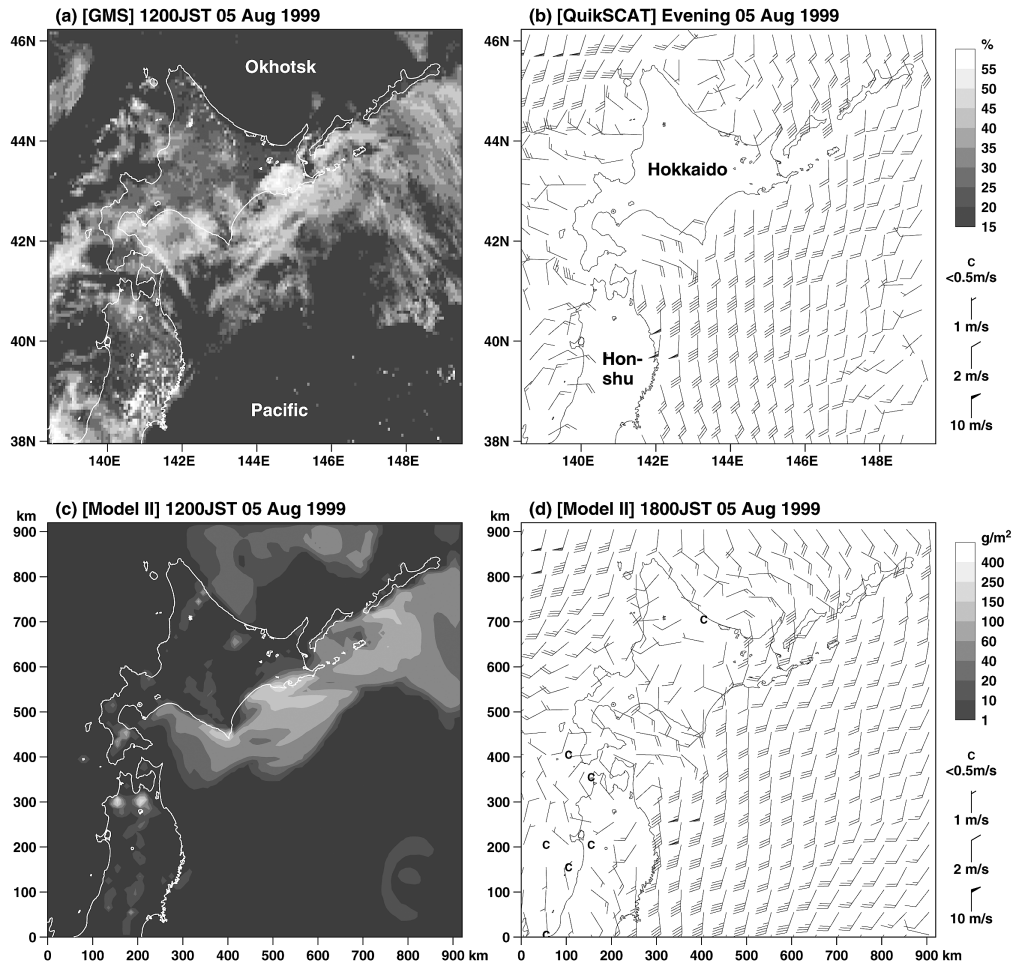


Fig. 2 Horizontal distributions of (a) albedo (%) at 1200 JST from GMS-5, (b) maritime winds (m s^{-1}) at about 1800 JST from QuikSCAT, and (c) LWP (g m^{-2}) at 1200 JST and (d) horizontal winds (m s^{-1}) at 10-m height at 1800 JST from Model II¹⁶⁾.

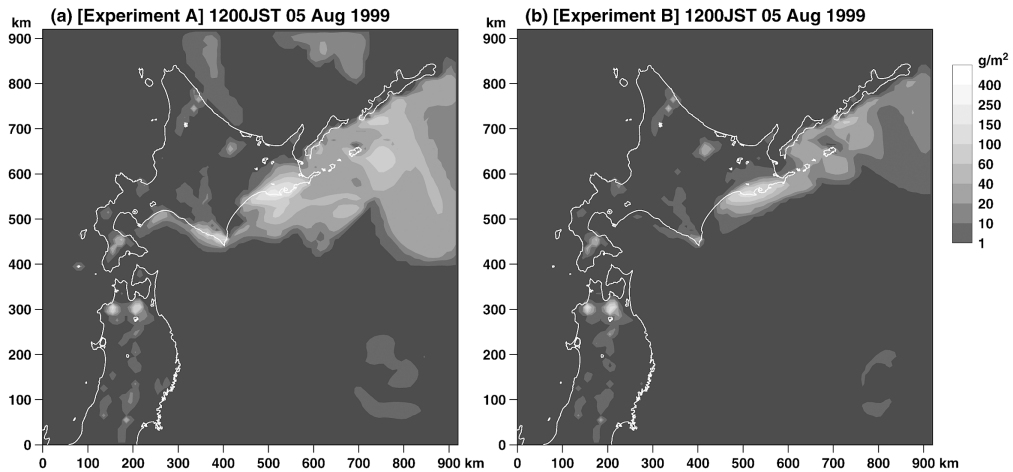


Fig. 3 Horizontal distributions of LWP (g m^{-2}) at 1200 JST from (a) Experiment A and (b) Experiment B. From the control run in Figure 2c, Experiment A replaces the NEAR-GOOS daily SST on 5 August 1999 with that on 10 August 1999, and Experiment B reduces the radiative heating/cooling rate by half¹⁶⁾.

References

- 1) Mellor, G. L. and Yamada, T., "Development of a Turbulence Closure Model for Geophysical Fluid Problems", *Rev. Geophys. Space Phys.* 20, 851–875, 1982.
- 2) Galperin, B., Kantha, L. H., Hassid, S., and Rosati, A., "A Quasi-Equilibrium Turbulent Energy Model for Geophysical Flows", *J. Atmos. Sci.* 45, 55–62, 1988.
- 3) Helfand, H. M. and Labraga, J. C., "Design of a Nonsingular Level 2.5 Second-Order Closure Model for the Prediction of Atmospheric Turbulence", *J. Atmos. Sci.*, 45, 113–132, 1988.
- 4) Gerrity, J. P., Black, T. L., and Treadon, R. E., "The Numerical Solution of the Mellor-Yamada Level 2.5 Turbulent Kinetic Energy Equation in the Eta Model", *Mon. Wea. Rev.*, 122, 1640–1646, 1994.
- 5) Janjić, Z. I., "Nonsingular Implementation of the Mellor-Yamada Level 2.5 Scheme in the NCEP Meso Model", Office Note No. 437, National Centers for Environmental Prediction, 61 pp, 2001.
- 6) Nakanishi, M., "Improvement of the Mellor-Yamada Turbulence Closure Model Based on Large-Eddy Simulation Data", *Boundary-Layer Met.* 99, 349–378, 2001.
- 7) Nakanishi, M. and Niino, H., "An Improved Mellor-Yamada Level-3 Model with Condensation Physics: Its Design and Verification", *Boundary-Layer Met.* 112, 1–31, 2004.
- 8) Musson-Genon, L., "Numerical Simulation of a Fog Event with a One-Dimensional Boundary Layer Model", *Mon. Wea. Rev.* 115, 592–607, 1987.
- 9) Kantha, L. H. and Clayson, C. A., "An Improved Mixed Layer Model for Geophysical Applications", *J. Geophys. Res.* 99(C12), 25235–25266, 1994.
- 10) Smagorinsky, J., Manabe, S., and Holloway, J. L., "Numerical Results from a Nine-Level General Circulation Model of the Atmosphere", *Mon. Wea. Rev.*, 93, 727–768, 1965.
- 11) Nakanishi, M., "A Lateral Boundary Condition Suitable for the One-Way Nesting Scheme", *Tenki* 49, 117–128, 2002 (in Japanese).
- 12) Klemp, J. B. and Durran, D. R., "An Upper Boundary Condition Permitting Internal Gravity Wave Radiation in Numerical Mesoscale Models", *Mon. Wea. Rev.* 111, 430–444, 1983.
- 13) Japan Meteorological Agency, "Outline of the Operational Numerical Weather Prediction at the Japan Meteorological Agency", Appendix to the WMO Numerical Weather Prediction Progress Report, Japan Meteorological Agency, Tokyo, 158 pp, 2002.
- 14) Katayama, A., "A Simplified Scheme for Computing Radiative Transfer in the Troposphere, Numerical Simulation of Weather and Climate", Technical Report No. 6, University of California, Los Angeles, 77 pp, 1972.
- 15) Nakanishi, M., "Large-Eddy Simulation of Radiation Fog", *Boundary-Layer Met.* 94, 461–493, 2000.
- 16) Nakanishi, M., and Niino, H., "An Improved Mellor-Yamada Level-3 Model: Its Numerical Stability and Application to a Regional Prediction of Advection Fog", *Boundary-Layer Met.* 119, 397–407, 2006.

改良版Mellor-Yamada レベル3モデルとその移流霧予報への応用

プロジェクト責任者

日比谷紀之 東京大学大学院理学系研究科

著者

中西 幹郎 防衛大学校

新野 宏 東京大学海洋研究所

改良したMellor-Yamada レベル3モデル(Nakanishi and Niino, 2004)の数値的安定性を改善した版を作成し、適用例として移流霧の領域予報を行なった。Mellor-Yamada レベル3モデルの数値的安定性を改善するためには、 L/q 、温度・水量の分散およびそれらの共分散について制限を課した。ここで L は乱流の支配長さスケール、 $q^2/2$ は単位質量あたりの乱流運動エネルギーである。数値的安定性を改善したモデルから得られる温度などの平均量の鉛直分布は、放射霧のラージエディシミュレーションで得られたものと同じ一致を示した。またこれを用いた領域予報実験では、衛星で観測された移流霧の水平分布をよく再現した。

キーワード：乱流クロージャモデル，移流霧の予報